

Abstracting Sparse DNN Acceleration via Structured Sparse Tensor Decomposition

Geonhwa Jeong
Georgia Institute of Technology
Atlanta, GA, USA
geonhwa.jeong@gatech.edu

Po-An Tsai
NVIDIA
Westford, MA, USA
poant@nvidia.com

Abhimanyu R. Bambhaniya
Georgia Institute of Technology
Atlanta, GA, USA
abambhaniya3@gatech.edu

Stephen W. Keckler
NVIDIA
Austin, TX, USA
skeckler@nvidia.com

Tushar Krishna
Georgia Institute of Technology
Atlanta, GA, USA
tushar@ece.gatech.edu

Abstract

Exploiting sparsity in deep neural networks (DNNs) has been a promising area to meet the growing computation need of modern DNNs. However, in practice, sparse DNN acceleration still faces a key challenge. To minimize the overhead of sparse acceleration, hardware designers have proposed structured sparse hardware support recently, which provides limited flexibility and requires extra model fine-tuning. Moreover, any sparse model fine-tuned for certain structured sparse hardware cannot be accelerated by other structured hardware.

To bridge the gap between sparse DNN models and hardware, this paper proposes tensor approximation via structured decomposition (TASD), which leverages the distributive property in linear algebra to turn any sparse tensor into a series of structured sparse tensors. Next, we develop a software framework, TASDER, to accelerate DNNs by searching layer-wise, high-quality structured decomposition for both weight and activation tensors so that they can be accelerated by any systems with structured sparse hardware support. Evaluation results show that, by exploiting prior structured sparse hardware baselines, our method can accelerate off-the-shelf dense and sparse DNNs without fine-tuning and improves energy-delay-product by up to 83% and 74% on average.

1. Introduction

DNNs have revolutionized various domains, such as computer vision [13, 30, 38], personal recommendation [44], speech recognition [4], and natural language processing [12, 54]. Meanwhile, DNN inference is also demanding more computation as they scale to billions of model parameters [8, 15, 60] and consume an enormous amount of input data [9, 34].

To address the increasing demand for DNN models, researchers propose to exploit *sparsity* in DNN models. Model pruning [19] is the most popular method to remove a set of parameters in the target DNN model based on certain criteria, inducing *weight sparsity*. This optimization exploits a phenomenon that empirically, large models are often overly parameterized and do not need all parameters to maintain the target accuracy at inference time. Deep learning (DL) model developers prefer to induce **unstructured sparsity** on weights

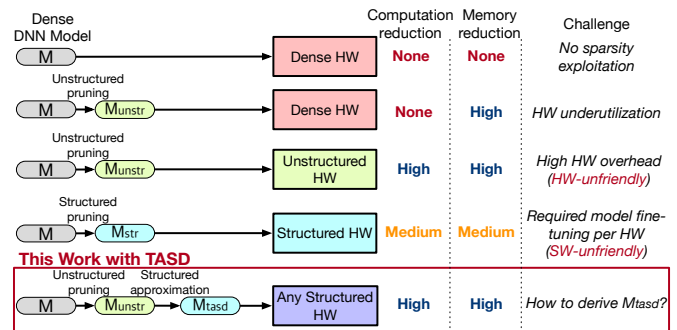


Figure 1: Different flows to exploit sparsity in DNNs.

so that they can focus on developing pruning algorithms to achieve better model accuracy and computation/model size trade-offs without any restriction. Also, many DNN models naturally exhibit *activation sparsity* due to the rectified linear unit (ReLU) that clips negative activation values to zeros, which induces unstructured activation sparsity.

As a result, early sparse DNN accelerators [50, 53, 64] target unstructured sparsity and can accelerate any sparse DNNs. Unfortunately, unstructured sparsity support is challenging to deploy as a specialized HW unit as it causes significant area and energy overhead for indexing logic and flexible distribution/reduction logic [27]. Without native HW support, unstructured sparsity in DNNs lead to irregular memory accesses and diverged control/execution patterns, which are hostile to parallel architectures like GPUs¹ and specialized tensor accelerators like tensor core and systolic array. This forces DNN model developers today to constrain the DNN sparsity search space to only consider coarse-grained *structured patterns*, such as channel or filter pruning [5, 42], while maintaining iso-accuracy, thereby, moving the burden to DNN model developers.

To balance the need, recently, hardware (HW) designers [27, 36, 46, 72] have proposed *fine-grained* structured sparsity support. Such designs force DNN developers to induce sparsity with certain constraints at a cost of achievable sparsity degree for iso-accuracy comparison, but promise predictable

¹The only sparse DNN accelerators on commercial devices is NVIDIA Sparse Tensor Core [46], which supports a fixed 2:4 structured sparsity.

performance gain on top of the existing DNN supports. For example, NVIDIA’s fine-grained 2:4 structured sparsity support balances the imposed constraints and achievable performance and provides a good target for DNN developers to optimize the network for. However, such methods impose an extra burden on DNN developers on top of the existing huge design space (DNN architectures, training recipes, etc.) to explore. Moreover, extending the existing support to more patterns [27, 62] means more overhead and design space exploration for both HW designers and DNN developers. We summarize different flows to exploit sparsity in Figure 1.

In this paper, we ask "Can we design a system to expose the flexible unstructured sparse interface to the DNN developers, but only with the efficient, less flexible structured sparse HW support?" Our answer is to introduce a new level of abstraction between DL model developers and hardware designers, similar to the abstraction layer in the instruction-set architectures. Specifically, we introduce a method, structured sparse tensor decomposition, to approximate any sparse tensor with a series of structured sparse tensors. Leveraging the distributed property of tensor algebra, we further propose to dynamically "decode" an unstructured sparse tensor algebra into a series of "microcode", i.e., structured sparse tensor algebra, which are efficient and compatible with prior structured sparse hardware.

We make the following contributions:

- We present the first work to bridge unstructured sparse DNN and structured sparse HW with Tensor Approximation via Structured Decomposition (TASD), which approximate any sparse tensor with a series of structured sparse tensors.
- We propose a framework, TASDER, which finds the TASD series for each DNN layer to accelerate dense/sparse DNNs with structured sparse hardware.
- We propose a simple architectural extension and dataflow on top of existing structured sparse accelerators [27] to execute TASD series efficiently.
- For various off-the-shelf dense and sparse DNNs, we show that TASD improves EDP by up to 83% and by 70% on average. We also show that across a range of DNNs, TASD can reduce the computation by 40%.

2. Background

2.1. Terminology

Sparsity is a characteristic of data that includes zero values. The sparsity degree of a given tensor is measured as the fraction of the number of zeros in the tensor to the number of the total elements in the tensor. If a tensor has 0% sparsity degree, we call the tensor *dense*. Sparsity by itself is often used to indicate sparsity degree. To describe the zero distribution in a tensor, a *sparsity pattern* can be given to the tensor. If there is no defined sparsity pattern, we call it *unstructured sparsity*. Various patterns can be classified as structured sparsity, such as block sparse [43], butterfly sparse [10], and mixed patterns [69].

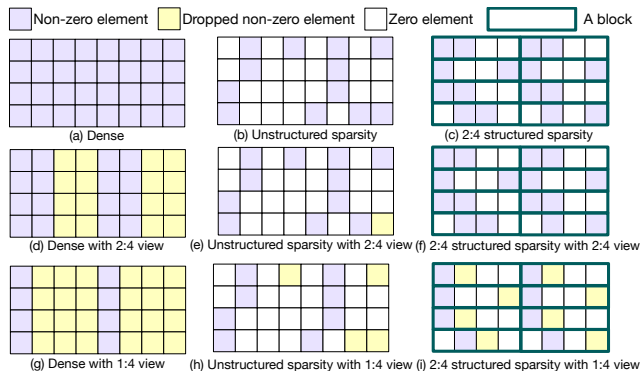


Figure 2: Different sparsity patterns and views.

One of the most popular pattern is **N:M structured sparsity** [71], as it is supported in both commercial product [46] and academia proposals [27, 36] with active training recipe research [67]. An N:M structured sparse tensor means that there can be at most N non-zeros in each M-element block in a certain rank of the tensor as shown in Figure 2.

A view of a tensor A for a sparsity pattern is a tensor after potentially dropping some elements to meet the rule of the sparsity pattern. For a matrix filled with non-zeros randomly, it is possible that the matrix does not meet the 2:4 sparsity pattern, i.e. there could be a block composed of 4 consecutive elements with more than two non-zeros. To generate a 2:4 view of the matrix, some non-zeros in the matrix should be dropped (pruned in DNNs) to meet the pattern. As this process could drop some original values, it can be *lossy*. Figure 2 also shows various tensors under different structured sparse views.

Prior work in DNN accelerators also proposed dense accelerators, unstructured sparse accelerators, 2:4 structured sparse accelerators, etc. To clarify the nomenclatures, in this paper, *if a sparsity pattern is used to describe a hardware accelerator, such accelerator should provide the lossless and native support for any input tensor under such view.*

2.2. DNN SW: Inducing sparsity in DNNs

Weight Sparsity. Without a specific pattern in mind, common model pruning methods introduces unstructured sparsity in weights [45]. Due to the irregular accesses to handle non-zeros in unstructured sparse matrices, unstructured sparsity is not adequate for accelerating DNNs on the existing parallel hardware, such as GPUs.

To address the issue, structured pruning forces pre-defined, static sparsity constraints in weights. For example, **N:M structured sparsity** [14, 25, 41, 62, 67, 70, 71] ensures that there are at most N non-zeros in each block composed of M consecutive elements, such that the required acceleration hardware can be trivial by exploiting the regularity in sparsity patterns. Thus, various accelerators, including recent sparse tensor cores in NVIDIA Ampere GPUs [46], target to exploit the fine-grained structured sparsity instead of unstructured sparsity. Nonetheless, structured pruning suffers from a higher loss of accu-

HW Support ↓	Dense Wgt	Unstr Wgt	Str Wgt	Dense Act	Unstr Act	Area Cost
Dense [28, 29, 47]	✓	✗	✗	✓	✗	✓✓
Unstr [50, 53, 64]	✗*	✓	✓	✗*	✓	✗
Str [27, 35, 46, 72]	✓	✗	✓	✓	✗	✓
TASD (This work)	✓	✓	✓	✓**	✓	✓

*With extra wiring/logic, unstructured sparse HW is inefficient if the tensor is dense.
**TASD enables further acceleration by approximating dense tensors with sparse tensors.

Table 1: Comparison of different DNN HW supports. Unstr: Unstructured sparse. Str: Structured sparse. Wgt: Weights. Act: Activations.

racy [16] than unstructured pruning since the extra pruning constraints reduce the flexibility. This extra loss of accuracy often leads to longer fine-tuning time (e.g., repeat the whole training process again) than unstructured sparse method to recover the loss in accuracy due to pruning [41].

Activation Sparsity. On the other hand, activation sparsity arises at runtime due to the non-linear activation functions such as ReLU, ReLU6 [22], and SquaredReLU [61], which clips negative values to zero. Activation sparsity is prevalent in both conventional Convolutional Neural Networks (CNNs) and recent Transformers [32]. Since it is intrinsic in DNN models, no extra fine-tuning or pruning steps are required to introduce activation sparsity. While the weight sparsity can be determined statically, activation sparsity is dynamic as the intermediate input feature map values depend on the inputs of the DNN model. Thus, the location of non-zeros and the degree of sparsity are unpredictable, similar to unstructured pruning, which makes it hard for structured sparse hardware to exploit input sparsity. Another challenge is that some recently proposed activation functions, such as GELU [21], and Swish [55], do not generate zero, which nullifies the benefits of exploiting activation sparsity in prior work [26].

2.3. DNN HW: Exploiting sparsity in DNNs

Table 1 shows the comparison of various sparse HW support for different DNN models. Prior unstructured sparse accelerators, including SCNN [50], SIGMA [53], Samsung NPU [26], and dual-side sparse core (DSTC) [64], target unstructured sparsity and skip redundant computations aggressively, but they suffer from non-trivial area/power costs due to the complex indexing and reduction logic, often introducing workload imbalance problems [37] as well. For example, SIGMA [53] introduces 37.7% area overhead compared to the dense baseline architecture due to its flexible and non-blocking distribution/reduction networks. Similarly, SCNN [50] and Griffin [59] produce 34% and 32% area overhead due to the support for the unstructured sparse dataflow. Moreover, when the sparsity degree is low or zero, they provide no improvement or even degrade performance and efficiency, due to the extra overhead for supporting unstructured sparsity.

More recent structured sparse tensor accelerator architectures, such as STA [35], Sparse Tensor Core from NVIDIA GPUs (NV-STC) [46], and VEGETA [27], provide HW support for structured sparsity with minimal area overhead. However, these designs accelerate **only structured pruned models**

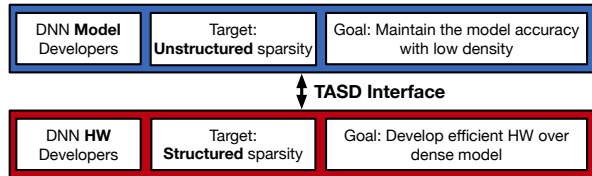


Figure 3: TASD Interface.

that use the specific pattern supported. Also, they focus on weight sparsity since it is not trivial to exploit unstructured activation sparsity without much overhead. Recently, S2TA [37] has tried to circumvent the challenge to support sparse activation by forcing structured sparse pattern dynamically, but it requires modifying the existing models and even more fine-tuning steps.

2.4. Tension between sparse DNN SW and HW

Figure 3 shows the state of sparse DNN software and hardware. On the one hand, model developers have shown that unstructured sparsity provides a better model accuracy and a higher sparsity degree. On the other hand, hardware developers have shown that structured sparsity support is more practical to include in GPUs and other DNN accelerators. Such tension in the desired sparsity patterns hampers the progress in bringing sparse DNN acceleration to practice.

The main drawback of the previous hardware-specific patterns is that the pruning software and hardware support are tightly coupled, such that the software generates a model specifically pruned for the pattern supported by the hardware. For example, a model pruned for the NV-STC can only be accelerated by NV-STC, not by S2TA. To decouple the tight relationship, we propose another layer of system software between the model developers and DNN hardware for sparsity. Our insight is to approximate a tensor by decomposing it into a series of structured sparse tensors. We leverage the distributive property in tensor algebra to execute the series of structured sparse GEMM. This mechanism thus provides an unstructured sparse interface for developers but only requires structured sparse support from hardware. As shown in Table 1, by bridging DNN model and HW, this work is able to accelerate all types of sparsity seamlessly with a low area overhead.

3. TASD: Tensor Approximation via Structured Decomposition

We introduce a method to **approximate unstructured sparsity using a series of structured sparsity**. In this paper, we use a set of N:M structured sparsities for TASD to explain the method and show how to use it practically, but the concept is general and not limited to only N:M structured sparse patterns.

3.1. Overview

We use an unstructured sparse matrix A to illustrate how TASD works in Figure 4. The matrix A has 6 zero elements out of 16

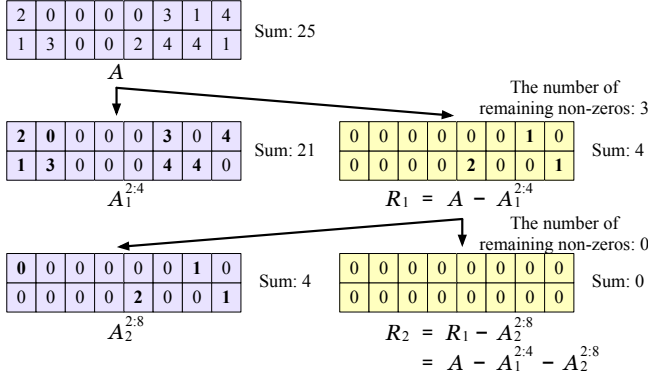


Figure 4: TASD example using a 2×8 matrix A .

total elements with a 37.5% sparsity degree. Also, note that the sum of all elements in A is 25.

Matrix A can be rewritten as a 2:4 structured sparse matrix (a 2:4 view of A) plus a remaining matrix, $A_1^{2:4}$ and R_1 , where $A_1^{2:4}$ is derived by extracting two **largest** elements out of four elements in each row in A while R_1 is the remaining matrix (i.e. $A - A_1^{2:4}$) after the extraction, as shown in [Equation 1](#).

$$A = A_1^{2:4} + R_1 \quad (1)$$

The extracted matrix, $A_1^{2:4}$ covers 70% in terms of the number of non-zero values while covering 84% in terms of the sum of the magnitudes. The percentage for the lost magnitudes is smaller than the percentage of the lost non-zero values because we extract two *largest* elements out of four consecutive elements. If we discard the remaining matrix R_1 , then the original matrix A can be *approximated* as $A_1^{2:4}$. Thus, we call this approximation **structured decomposition**. If we approximate A with a 3:4 pattern instead of the 2:4 pattern, we can derive matrix $A_1^{3:4}$ with a structured decomposition that drops only one non-zero element, covering 90% of the number non-zeros and 96% of the sum of total magnitudes.

Instead of using a denser N:M, we can further decompose R_1 using another structured pattern, such as 2:8. A_2 can also be derived by extracting two largest elements out of **eight** consecutive elements in R_1 , making A_2 as a 2:8 structured sparse matrix. Similar to the previous decomposition, we call the remaining matrix R_2 as shown in [Figure 4](#). All elements of A are covered by $A_1^{2:4}$ and $A_2^{2:8}$, so A is equal to $A_1^{2:4} + A_2^{2:8}$, thus the approximation of A to $A_1^{2:4} + A_2^{2:8}$ is lossless. Since the unstructured sparse matrix is approximated using a set of structured sparse matrices, we call this method as Tensor Approximation via Structured Decomposition (TASD).

Theoretically, structured decomposition can have infinite terms. Below, we formalize the process more generally using different structured sparse patterns denoted as s_i .

$$A \simeq A_1^{s_1} + A_2^{s_2} \quad (2)$$

$$\simeq A_1^{s_1} + A_2^{s_2} + A_3^{s_3} \dots + A_n^{s_n} \quad (3)$$

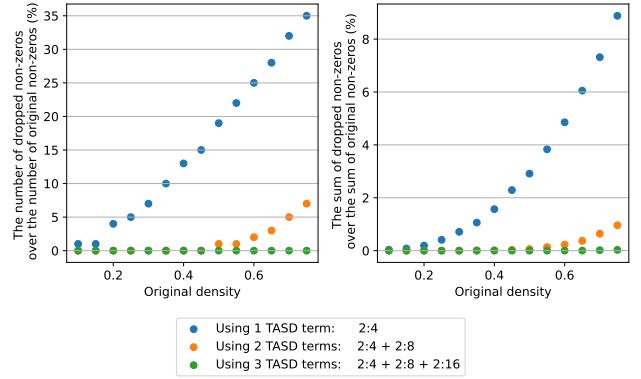


Figure 5: Percentages of dropped non-zeros and the sum of dropped non-zeros after applying different TASD series.

We call A as the original matrix and $\sum A_i^{s_i}$ as **TASD series**, to draw an analogy to the classic Taylor series²: Each successive term (residual structure sparse tensor) improves the accuracy of the approximation. A TASD series configuration includes the number ("order") of TASD terms (n) and the structured sparsity pattern (s_i) for each TASD term. Using TASD, one can generate a structured sparse view of a given tensor, and the error between the view and the original tensor would depend on the TASD series configuration.

Using TASD for Matrix Multiplication: TASD decomposes any tensor A into a series of structured sparse tensors. The decomposed tensors can be used in any tensor algebra, such as matrix multiplication ($C = A \times B$), which can be approximated as $A_1^{s_1} \times B$, so if s_1 is 2:4, and the matrix multiplication is running on NVIDIA STC, potentially 50% of Multiply-and-Accumulate (MAC) operations could be skipped.

With the distributive property of tensor algebra, matrix A can be approximated using more TASD terms such as $(A_1^{s_1} + A_2^{s_2})B = A_1^{s_1}B + A_2^{s_2}B$. If s_1 is 2:4 and s_2 is 2:8, about 25% of MAC operations could be skipped. Thus, finding the proper TASD series to minimize the error while maximizing compute reduction will determine the quality of the approximation.

3.2. An analysis of TASD with synthetic data

The number of dropped non-zeros and the sum of the dropped magnitudes are crucial as they correlate to the potential loss of accuracy when applying TASD. Thus, we first conduct preliminary experiments with synthetic data using various TASD series and matrices to understand the trade-offs.

We generate a synthetic matrix B with dimensions of 128×128 and densities ranging from 0.1 to 0.75. We explore three TASD series in this experiment; 1) using one term with 2:4, 2) using two terms with 2:4 and 2:8, and 3) using three terms with 2:4, 2:8, and 2:16. To consider various distributions, we tested two different distributions, a uniform random distribution between 0 and 1 and a normal distribution with a

²Taylor series approximates any function with polynomials, while TASD series approximates any tensor with structured sparse tensors.

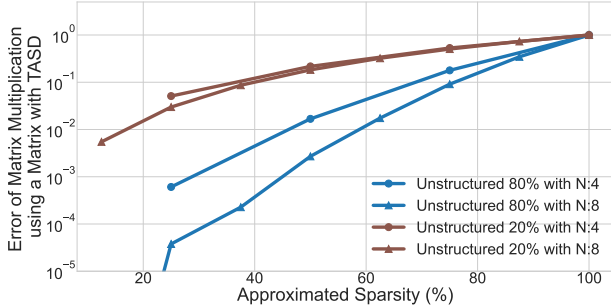


Figure 6: The error between the result from the original matrices and the result with an approximated matrix using TASD assuming different sparsity in the original matrix.

mean of 0 and a standard deviation of $\frac{1}{3}$. Figure 5 shows the results with matrices generated using the normal distribution.

Takeaways: 1) If the matrix is very sparse, the percentage of dropped non-zero values becomes noticeably small, less than 1%, even with just two TASD terms. 2) Since we choose elements with a greedy approach (i.e., keep the largest non-zero), the percentage of dropped total magnitude is lower than the percentage of dropped non-zero values, allowing better approximation even for higher densities.

In addition, we also find that across different distributions, percentages of dropped non-zero values are similar since they depend on the density of the original matrix, but percentages of the dropped total magnitude vary slightly. Interestingly, we observed that Mean Square Errors (MSEs) vary significantly depending on the distribution. This implies that not the sparsity degree only, but the actual distribution is also critical for finding a high-quality TASD series configuration.

Using TASD for Matrix Multiplication: To understand the impact of using TASD for matrix multiplication, we run another experiment using matrices A and B with the dimensions of 256×256 . We set each element to have a random value between 0 and 1. For matrix A, we generate unstructured sparsity with two sparsity degrees 20% and 80%, and we keep B as dense. Then, we apply one-term TASD on A with 0-4:4 and 0-8:8 TASD configurations. We measure the error as the Frobenius norm of the result with approximated operands divided by the original Frobenius norm, $\frac{\|(A-A^*)B\|}{\|AB\|}$. We represent configurations with *approximated sparsity*, which means the sparsity degree of a structured sparse pattern. For example, 1:4 pattern and 2:8 pattern both have an approximated sparsity of 75%. We plot the errors with different TASD configurations and approximated sparsity degrees in Figure 6.

Error Behavior: The first trend we observe is that the error gets smaller as the approximated sparsity gets lower since it is likely to drop fewer non-zeros with a more conservative approximation. Second, for the same approximated sparsity and the block size (M), the error gets smaller as the matrix A gets sparser. Given the same TASD configuration, the sparser matrices would drop fewer non-zeros using the same TASD configuration as shown in Figure 5, thus resulting in a smaller

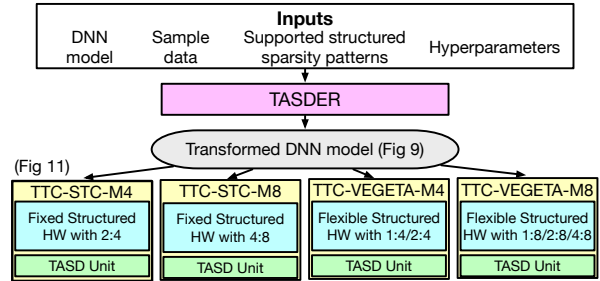


Figure 7: System overview with TASDER.

error. Third, with the same sparsity of matrix A and approximated sparsity, the N:4 configuration causes a larger error than the N:8 configuration (such as 1:4 and 2:8), since the expressiveness of the N:8 pattern is higher. Finally, given any unstructured sparse tensor, *we can limit the error of matrix multiplication by conservatively selecting the TASD configuration, while maximizing the compute reduction*. This optimization thus becomes the key to leveraging TASD for accelerating sparse DNN models with structured sparse hardware.

4. HW/SW Co-Design with TASD

In Section 3, we introduce our approximation method, TASD, in general. In this section, we show how our method can be used to accelerate DNN models with sparse weights and inputs. Although TASD can also be used to accelerate the DNN training, we focus on how to accelerate DNN inference in this work. There are two main insights that inspired us to use TASD for DNN inference.

- 1) By its nature, DNN models are able to tolerate small errors in their internal computations.
- 2) Although TASD is a lossy approximation method, carefully selected TASD terms can provide high-quality approximations with a limited number of non-zeros being dropped.

4.1. System architecture overview

We introduce our optimizer system, TASDER, which takes a DNN model, sample data, target HW information including structured sparsity patterns, and hyperparameters as shown in Figure 7. Internally, TASDER will search for the TASD configuration for each layer of the given DNN model and return the configurations. In the following subsections, we introduce TASD-W and TASD-A, which are the methods to exploit TASD on weights and activations, respectively. We also explain how the TASD configuration per layer is selected in our framework. In this work, we only consider convolution (CONV) and fully-connected (FC) layers in DNN models to apply TASD as they usually consume most of the execution cycles, and they get converted to matrix multiplication operations using algorithms such as `im2col` for parallelization.

4.2. TASD-W: Applying TASD on weights

We expose an unstructured interface to ML model developers as the target of optimization so that they can focus on the

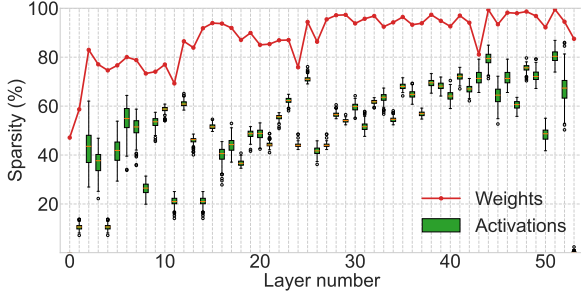


Figure 8: Sparsity degrees for each layer in 95% unstructured sparse ResNet50 from SparseZoo.

techniques to prune their models as much as possible without considering any specific HW-friendly sparsity pattern. Therefore, the optimization problem for TASD-W is that given the weights of DNN models as unstructured sparse tensors, use the available structured sparse HW to accelerate the model execution as much as possible.

We assume that the target hardware can accelerate the structured sparsity patterns, S_1, \dots, S_n . A TASD configuration of the i th layer, C_i , is a sequence of S . For a given DNN model M , a TASD transformation of the model, T , is defined as applying a sequence of C_i where C_i is the TASD configuration for each layer in the model. Then, the target is to find a TASD transformation T_{opt} for a given model where

$$T_{opt} = \underset{T}{\operatorname{argmin}}(\operatorname{Latency}(M_T)) \quad (4)$$

$$\text{such that } \operatorname{Accuracy}(M_T) \approx \operatorname{Accuracy}(M_{original}) \quad (5)$$

A simple way to use TASD-W is using the same TASD configuration for all layers in the model, i.e. applying **network-wise TASD-W**. As the number of supported structured sparsity patterns, n , is not large enough, the T_{opt} for network-wise TASD-W could be found with the exhaustive search.

A better method to use TASD-W is using different TASD configurations for different layers, i.e. **layer-wise TASD-W**. The TASD transformations that can be covered by layer-wise TASD-W is a super-set of the TASD transformations in network-wise TASD-W. Usually, a pruned model with unstructured sparsity does not guarantee the same sparsity across layers, i.e. even though the overall sparsity is 95% for the model, different layers could have different sparsity degrees as shown in Figure 8. Unlike network-wise TASD-W where all the layers use the same TASD configuration, it is not straightforward how to choose a TASD configuration per layer as there could be numerous options per layer. To minimize the accuracy drop, it is crucial to reduce the number of dropped non-zeros after applying TASD, which would prefer conservative TASD configurations. On the other hand, to maximize the performance gain, it would be better to apply aggressive TASD configurations, which would be able to be translated into higher sparsity and efficiency gain.

To address this, we design and implement a greedy-based algorithm that optimizes across all layers. This greedy al-

gorithm first measures the percentage of dropped non-zero elements of each TASD configuration for all layers and sorts the configuration-layer pairs by their percentage of dropped elements. Next, it greedily applies the TASD configuration based on the sorted order until the model quality is $<99\%$ of the original model (i.e., prioritize the option with the smallest dropped non-zeros). Since it only takes a single pass to all layers, the runtime overhead is trivial (a few seconds per model), while the extra training needed for structured sparse HW often takes hundreds of GPU hours [62].

We use TCONV/TFC to indicate a CONV/FC layer with TASD as shown in Figure 9, and the TASD configurations found above would be applied to the corresponding TCONV/TFC layers. In Figure 9 (a), we show how the conventional CONV/FC layer works with unstructured sparse activations (usually from ReLU) with dense weights. In Figure 9 (b) shows how a TCONV/TFC layer works with unstructured sparse weight. TASDER would modify unstructured sparse weights to structured sparse weights with TASD-W.

4.3. TASD-A: Applying TASD on activations

TASD can also be applied to activations to improve a DNN execution as shown in Figure 9 (c). Unlike weights which are static, TASD should be applied for dynamic decomposition during the runtime as activations are dynamic. In Figure 10 (a) and (b), we show a baseline ResBlock and a ResBlock with TCONV and TASD layers, which decompose activation tensors with given TASD configurations. We add TASD layers after ReLU layers so that they can minimize the number of dropped non-zeros after approximation. The same can be applied to a Transformer Block, where the FC layers in the multi-layer perception module can be replaced with TFC by inserting a TASD layer before TFC layers as shown in Figure 10 (c) and (d). Ideally, other FC layers in a Transformer Block could also be replaced with TASD and TFC layers, but empirically we found it hard to maintain the model quality.

Similar to TASD-W, the simplest way to choose a TASD configuration for each TASD layer is using network-wise TASD where all TASD configurations are same across all TASD layers. Assuming limited supported structured sparsity patterns from HW, only a handful number of options need to be explored. However, similar to weights, this may not be efficient as activations from different layers show significantly different degrees of sparsity, as shown in Figure 8.

To address this issue, we again leverage layer-wise TASD as it can tailor the TASD configuration to each layer. However, unlike the TASD-W, it is not feasible to test every option for each layer to find out the best options as the target tensors (activations) are dynamically generated.

Nonetheless, we find that a small set of calibration dataset (e.g., 1000 images for ImageNet [11]) can provide enough insights. As shown in Figure 8, while different layers have different sparsity degrees, for a particular layer, the activation sparsity degree remains in a small range across different input

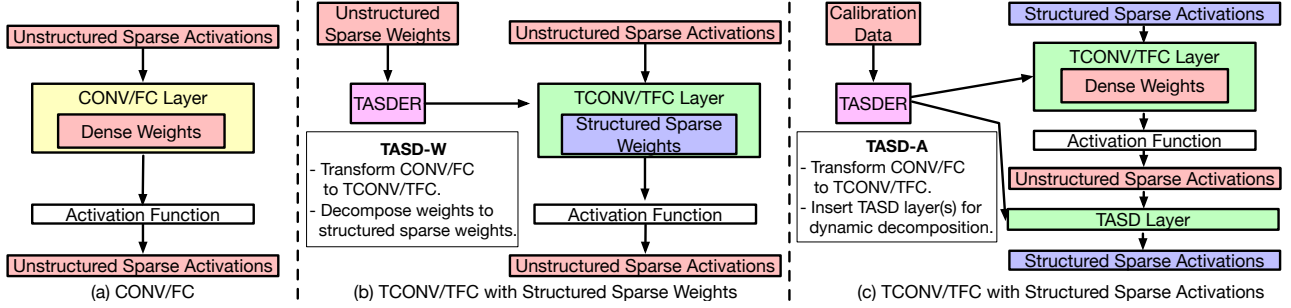


Figure 9: Comparison of flows of an original model with a conventional CONV/FC layer and transformed models with a TCONV/TFC layer with structured sparse weights, and a TCONV/TFC/TASD layer with structured sparse activations.

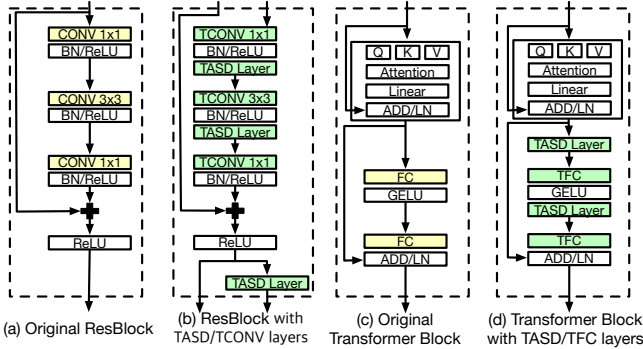


Figure 10: ResBlocks with CONV and TASD/TCONV and Transformer Blocks with FC and TASD/FC.

images. Therefore, TASDER takes calibration data as an input, so it can profile the given DNN model with the calibration data and collect the statistics (e.g., average, 99th percentile) about activation sparsity per layer.

To choose a TASD-A configuration for each layer, we use a *sparsity-based* selection method, instead of the non-zero-based method for TASD-W. We use a hyperparameter, α , to tune the aggressiveness of the TASD approximation. For a given layer L_i and the available configurations in the target HW (e.g., H_1, \dots, H_4), we choose C_i as H_j where j is the largest integer where $S(L_i) + \alpha > H_j$. If we use a larger α , we choose the TASD configuration more aggressively (i.e. allowing more dropped non-zeros). We summarize the algorithm in Listing 1.

Listing 1: The sparsity-degree-based TASD selection.

```

1 target_sparsity = sparsity + alpha;
2 if (target_sparsity > H[3])
3   return H[3];
4 else if (target_sparsity > H[2])
5   return H[2];
6 else if (target_sparsity > H[1])
7   return H[1];
8 else if (target_sparsity > H[0])
9   return H[0];

```

Beyond sparsity: Supporting non-ReLU-based DNNs. ReLU-based DNNs naturally induce sparsity in activation tensors, so by collecting the sparsity statistics, TASD-A can find the appropriate configuration for each layer. However, for better accuracy, state-of-the-art DNNs have replaced ReLU with

Pattern	TASD series	Pattern	TASD series
1:8	1:8	5:8	4:8 + 1:8
2:8	2:8	6:8	4:8 + 2:8
3:8	2:8 + 1:8	7:8	-
4:8	4:8	8:8	Dense

Table 2: Supported sparse patterns with TTC-VEGETA.

other activation functions, such as GeLU [21] and Swish [55], which do not induce any sparsity in activations making the activations dense. Thus, our sparsity-degree-based TASD selection (Listing 1) to choose TASD configuration for TASD-A for each layer would not work for those DNNs.

To address this, we investigate the distribution of the magnitude of all elements in the activation tensors from GeLU/Swish-based DNN. We found that, while no element in the tensor is exactly zero, a huge number of elements have tiny magnitude, compared to the range of magnitude for all elements. Therefore, we let TASD-A leverage this skewed distribution and collect the magnitude statistics. We introduce another heuristic, *pseudo-density*, which aims to preserve a fixed percentage (e.g., 99%) of the sum of all elements in a tensor, to determine the best TASD configuration for every layer. Using the pseudo-density for the non-ReLU-based DNNs, we can use the same sparsity-degree-based method (Listing 1) (i.e. by replacing *sparsity* to $1 - \text{pseudo-density}$).

The approximating nature of TASD allows the system to also accelerate non-ReLU-based DNNs, while prior work that specifically targets activation sparsity cannot.

4.4. Structured sparse HW for TASD

TASD works best when there are at least a few supported structured sparse patterns in the target sparse accelerator. While the TASDER optimizer is HW-agnostic, we propose to build on top of a recently proposed flexible structured sparse tensor accelerator to maximize the benefit. Inspired by previous structured sparse accelerators [27, 36, 46], we introduce TASD Tensor Core (TTC). We adopt a design similar to VEGETA [27] engine composed of multiple processing elements (PEs) while providing support for 1:8, 2:8, and 4:8 structured sparse patterns, and we call it TTC-VEGETA. With TASD and a limit of up to 2 terms, a TTC-VEGETA engine can support

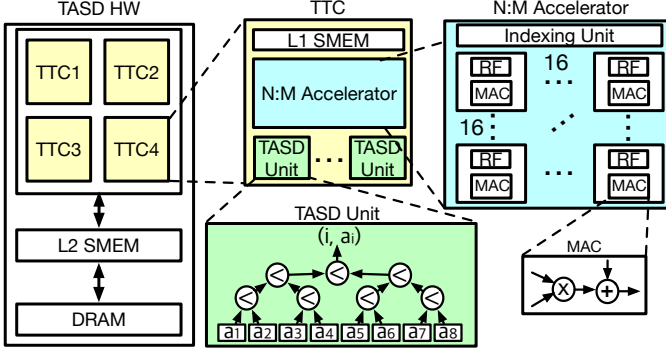


Figure 11: TASD-HW composed of four TTCs.

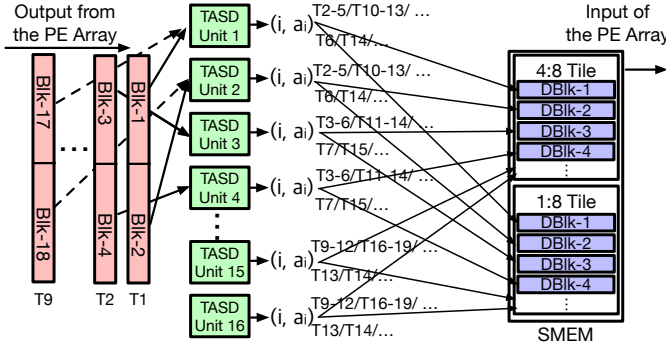


Figure 12: Dataflow between PE array and TASD units.

7 out of all the N:8 patterns³ as shown in Table 2 even though the original VEGETA supports only three sparse patterns.

Note that TTC can adopt other structured sparse designs, such as STC [72] with supports for 2:4 and dense, which we call TTC-STC. This would limit the flexibility in approximation using TASD compared to VEGETA-based TTC design, but TASDER is still able to optimize some layers. We explore the benefit of flexibility in Section 5.

In Figure 11, we show the overall design of a TASD HW that is composed of four TTCs similar to the one used in the previous work [66]. The only modification we add on top of the N:M accelerator such as STC or VEGETA, is the TASD units (shown in the right part of Figure 11) that dynamically extract TASD terms from the activation tensor, similar to the DAP unit in the recent S2TA [37] accelerator. TASD-W can be applied offline through pre-processing since weights do not change during the runtime, but TASD-A requires the TASD unit as activations will be dynamically generated at runtime.

Given the computation latency on TTCs, the minimum number of TASD units per TTC required to hide the latency of TASD units depends on the mapping and TTC implementations. For example, each TTC-VEGETA with $M=8$ generates 16 (number of PE columns in each TTC) output elements per cycle (i.e. 2 blocks per cycle) as shown in Figure 12, which will be fed to TASD units. For an M -element block, a TASD unit sequentially extracts the largest values, so the decomposi-

³The 7:8 pattern needs 3 TASD terms and is rarely used in practice.

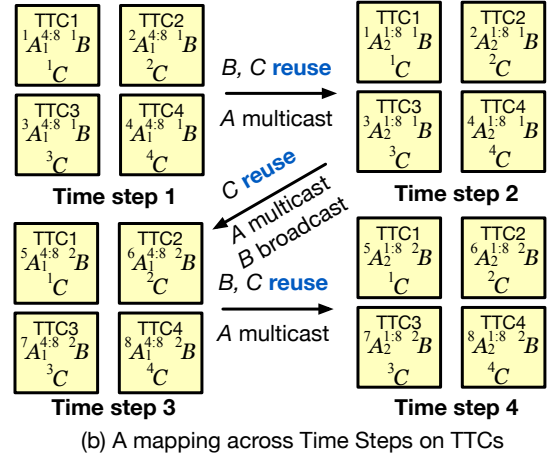
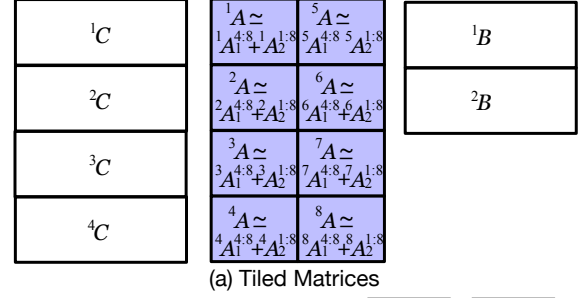


Figure 13: A mapping of matrix multiplication on TTCs.

tion takes up to M cycles for any TASD configuration as the sum of N_s in a TASD configuration cannot be larger than M .

The example in Figure 12 uses TASD configuration composed of 4:8 and 1:8, so it takes 5 cycles per block. At T1 (cycle 1), two blocks (Blk-1, Blk-2) will be produced from the PE array and Blk-1 and Blk-2 will be processed by TASD Unit 1 and TASD Unit 2, respectively (each cycle, two TASD units start execution). During T2-T5, Blk-1 and Blk-2 will be used to extract Decomposed Blocks, DBlk-1 and DBlk-2 for 4:8 Tiles. Then, during T6, DBlk-1 and DBlk-2 for 1:8 Tiles will be generated and stored. The decomposed blocks will be used as the inputs of the next layer. With 16 TASD units, a TTC-VEGETA can operate without stalls on the PE array due to the decomposition as a TASD unit is always guaranteed to be available after M cycles (i.e. by Little's law, $16 = 2 \times 8$). We also measure and present the area overhead for TASD units in Section 5.

Decomposition-aware dataflow. In Figure 13, we show a mapping of a matrix multiplication with an approximated matrix A using a TASD configuration, 4:8 and 1:8 for the TTC. We first show how we tile the matrices and how they are mapped in the private register file and shared buffer of each TTC. When matrix A is decomposed into two TASD terms, A_1 , and A_2 , the original matrix multiplication can be approximated as the sum of the two matrix multiplications and accumulation ($A_1 \times B + A_2 \times B$). As the two matrix operations share the same input B and partial sum C , we **keep B tiles in the L2 Scratchpad Memory (SMEM) and C tiles stationary in**

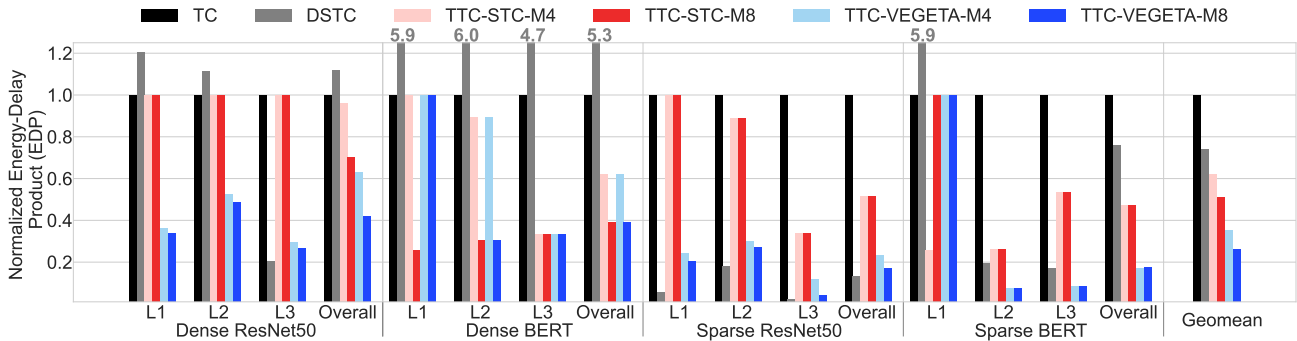


Figure 14: Energy-delay-products for running dense and sparse ResNet50 and BERT. For TTC-STC and TTC-VEGETA, we use the TASD transformations found from TASDER. M4/M8 represents design with N:4/N:8 supports.

HW Design	HW Sparsity Support
TC	None
DSTC	Unstructured
TTC-STC-M4	2:4 (TASD 1T)
TTC-STC-M8	4:8 (TASD 1T)
TTC-VEGETA-M4	1:4, 2:4 (TASD 1T) + 3:4 (TASD 2T)
TTC-VEGETA-M8	1:8, 2:8, 4:8 (TASD 1T) + 3:8, 5:8, 6:8 (TASD 2T)

Table 3: Summary of different HW designs. TASD 1T and 2T indicates using TASD 1 term and 2 terms, respectively.

Model	Weight	Activation	Layers Dimensions
Dense ResNet50 (ReLU-based)	Dense	Sparse	L1: M784-N128-K1152 L2: M3136-N64-K576 L3: M196-K2304-N256
Sparse ResNet50	Sparse	Sparse	
Dense BERT (GeLU-based)	Dense	Dense	L1: M768-N128-K768 L2: M3072-N128-K768
Sparse BERT	Sparse	Dense	L3: M768-N128-K3072

Table 4: Representative layers from the target workloads. L1, L2, and L3 are representative layers. We use "Overall" for the entire network.

the L1 SMEM of TTC while changing decomposed A tiles to temporally reuse B and C tiles for data reuse (between timestep 1 and 2, timestep 3 and 4 in Figure 13 (b)). For each accelerator tile, (i.e. for each timestep), we **keep each element of A tile stationary in the register file of each PE** for the temporal reuse, while the B and C elements are mapped correspondingly. By increasing the tile size for GEMM-N dimension, the reuse count for A tile at PE level could increase, which is limited by the size of the capacity of each SMEM. We swap C tiles at the very end to minimize the number of write-back operations to other levels. Although we maximize reuses for decomposed tiles, there is still unavoidable overhead such as reading C tiles again, but this is insignificant compared to the energy saving by skipping ineffectual computations using TASD. In Section 5.5, we quantify the energy overhead.

5. Evaluation

5.1. Methodology

TASD accelerates both sparse and dense DNNs *without fine-tuning*, so we evaluate TASD-W on sparse DNNs from SparseZoo [45] and TASD-A on dense DNNs from TorchVision [1]. We use a classic convolutional network, ResNet50 [20], and a transformer-based network, BERT [12], to illustrate detailed trade-offs between accuracy and performance. For the baseline HW, we compare against dense tensor core (TC) [46] and dual-side sparse tensor core (DSTC) [64] as representative dense and unstructured sparse accelerators. We configure these baselines as in the Sparseloop Artifacts [2]. We use 4 variants of TTC, based on STC and VEGETA, and with N:4

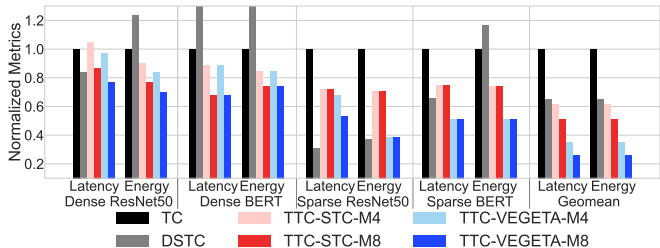


Figure 15: Latency and energy for various designs.

and N:8 designs, to show the extra benefits of TASD from the flexibility of the structured sparse hardware as summarized in Table 3. All designs use the same memory hierarchy and the same amount of PE (MACs) to ensure a fair comparison.

To evaluate the effectiveness of different TASD methods on a target accelerator, we develop TASDER as a framework to search for TASD transformations and calculate the accuracy of the model with each TASD transformation using PyTorch [51]. Following the requirement in MLPerf [56] inference benchmark, we only consider a model as valid with TASD if the model still achieves an accuracy higher than 99% of the accuracy from the original model. Next, we run each DNN layer with the given TASD series configuration using Sparseloop [66], a sparse tensor accelerator modeling framework to obtain per-layer results and aggregate the result for the entire network, which is consistent with prior accelerator simulation frameworks [24, 31, 40, 49, 58]. We simulate all layers in the networks, but to show per-layer results as well as the full network result ("Overall"), we also chose three

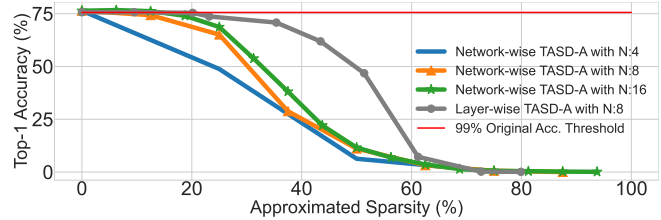
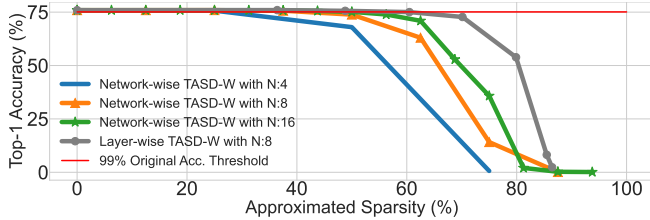


Figure 16: Network-wise and Layer-wise TASD on ResNet50. Left: TASD-W. Right: TASD-A.

representative layers (from early, mid, late) for each DNN as shown in Table 4. Also, to show the applicability of TASD for other sparse and dense DNNs, we evaluate the theoretical MACs reductions for another 8 DNNs, similar to prior work in pruning algorithms for structured sparse patterns [7, 62].

5.2. DNN acceleration with TASD

Figure 14 shows the energy-delay product (EDP) for the 4 workloads on various DNN accelerators, normalized to the dense TC.

Even though DSTC is able to exploit unstructured sparsity, the overhead of unstructured sparse acceleration (such as accessing accumulation buffer frequently) offsets the benefit and even outweighs the benefits when the workload has only one sparse operand or there is no sparse operand, causing 12% and 167% **larger** EDP for dense ResNet50 and dense BERT while reducing EDP by 55% for sparse BERT. DSTC works best for sparse ResNet50 and improves EDP by 87%, as both weight and activation tensors are unstructured sparse with a high sparsity degree (95% sparse weight). Overall, it is able to reduce 35% across all workloads on average.

Unlike DSTC, TASD-based TTC accelerators improve EDP over the TC baseline for all workloads. With the flexibility in sparsity patterns, TTC-VEGETA-M8 improves EDPs for all workloads, by 58%/61% for dense ResNet50/BERT and 83%/82% for sparse ResNet50/BERT. Even with only one fixed structured sparsity pattern, TTC-STC-M4 improves by 4%/32% for dense ResNet50/BERT and 49%/53% for sparse ResNet50/BERT. This result shows that TASD can effectively leverage structured sparse hardware for off-the-shelf dense and sparse DNNs with no fine-tuning, and the extra flexibility (increasing M) in the baseline accelerator increases the benefit.

Figure 15 provides more details in end-to-end latency and energy consumption for various designs. TTC-VEGETA-M8 is always the most energy-efficient design across all workloads and is slightly slower than DSTC only for sparse ResNet50 (by 22%). This result shows TASD provides a better overall tradeoff than unstructured sparse accelerators, especially considering their high area overheads.

5.3. Analysis of TASD

Network-wise vs. layer-wise TASD. The left plot of Figure 16 shows the impact of network-wise TASD-W on the top-1 accuracy of unstructured sparse ResNet50 (95% sparsity). We applied network-wise TASD-W with N:4, N:8, and

N:16 structured sparsities. For example, the network-wise TASD-W with 2:4 uses one TASD term with the 2:4 pattern to the weights of all convolution and fully-connected layers in the sparse ResNet50. Since TASD is a lossy method as shown in Section 3.2, aggressive TASD series approximation can result in a notable accuracy drop. Among different N:4, N:8, N:16 options, we found that 3:4, 5:8, 10:16 is the most aggressive approximation among the available options while meeting the 99% accuracy requirement. Especially, using network-wise TASD-W 5:8 (4:8 + 1:8 for TTC-VEGETA) and power gating for sparse activations, compared to the dense baseline, we observe it achieves 24% and 53% reduction in cycle and energy respectively, thus reducing 75% EDP for Sparse ResNet50.

Using different TASD series configurations for different layers is more effective as it can adjust the aggressiveness for each layer. To choose a TASD configuration per layer, we use the sparsity-based selection method that we introduce in Section 4.2. By changing the hyperparameter alpha, we are able to adjust the aggressiveness of our approximation method. As layer-wise TASD-W can be adaptive to each layer, the overall approximation can be applied more aggressively. As a result, compared to the dense baseline, we observe 47% and 61% reduction in energy and cycle respectively, thus reducing 83% EDP for Sparse ResNet50.

In the right plot of Figure 16, we show the top-1 accuracy when network-wise and layer-wise TASD-A is applied with different TASD series. Similar to TASD-W, layer-wise TASD-A is more effective than network-wise TASD-A. However, the accuracy loss due to approximation shows up with a much smaller approximated sparsity. As shown earlier in Figure 8, the sparsity degree is larger in weights compared to that in activations for sparse ResNet50. Thus, the same TASD series drops a larger portion of non-zeros in TASD-A than TASD-W, incurring a higher loss of accuracy.

TASD on more DNN models.

To further investigate the impact of TASD-W on different sparse DNNs, we applied layer-wise TASD-W on different Sparse ResNet and VGG families with a requirement to maintain 99% of the original accuracy. We use the pre-trained unstructured sparse models from SparseZoo [45]. Across different sparse ResNet models and VGG models, TASD-W reduced 49% MAC operations while maintaining 99% accuracy, as shown in Figure 17. On the other hand, to understand the potential impact of TASD-A on other DNN models, we applied TASD-A on various models including both convolu-

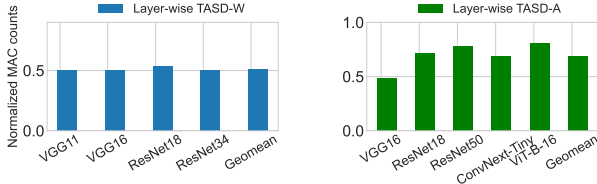


Figure 17: Layer-wise TASD on more DNN models. Left: TASD-W. Right: TASD-A.

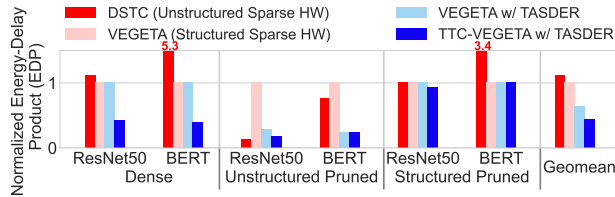


Figure 18: Study on DSTC, VEGETA, TASDER, and TTC with different types of models.

tion networks and a transformer-based network, as shown in Figure 17. We use the pre-trained dense models from TorchVision [1] and Huggingface for this evaluation and we use the requirement to meet 99% of the original accuracy. We observe that the layerwise TASD-A is effective for various models and achieves 32% reduction in MACs for other models on average.

5.4. Comparison against structured sparse accelerators

To study how the proposed TTC-based accelerator compared to prior structured sparsity accelerators, we conduct an ablation study to show how different novelties in this work contribute to the efficiency gain. Figure 18 shows the normalized EDP improvement for four different system: DSTC, VEGETA without TASDER, VEGETA with TASDER, TTC-VEGETA with TASDER. Without TASDER and HW-aware fine-tuning, VEGETA cannot exploit sparsity in off-the-shelf DNNs and has no improvement at all. If the model is structured pruned using HW-aware fine-tuning, VEGETA can exploit sparsity achieving a comparable EDP to TTC-VEGETA. With TASDER, VEGETA can exploit weight sparsity in unstructured sparse ResNet50/BERT since TASDER transforms unstructured sparse weights into structured sparsity supported by VEGETA. Finally, with dynamic decomposition support for activation sparsity, TTC-VEGETA can also exploit activation sparsity, further improving EDP for all DNNs.

5.5. Energy overhead due to TASD

Figure 19 shows the energy breakdown for a representative layer from sparse ResNet50 for dense TC and TTC-VEGETA with a TASD configuration of 4:8+1:8. TTC-VEGETA exploits sparsity and saves energy consumption at all levels of the architecture, which saves 55% energy over the dense TC. Moreover, the decomposition-aware dataflow in Section 4 min-

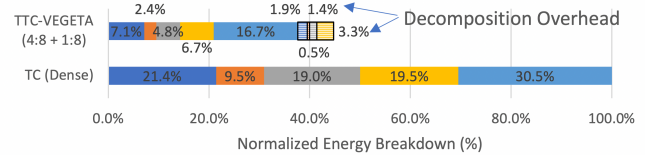


Figure 19: Energy Breakdown: TTC vs. Dense TC.

imizes decomposition overheads by accessing the RF (with C reuse) and SMEM (with B reuse) instead of accessing DRAM.

5.6. Area overhead of the TASD unit

We also measured the area overhead to support TASD on top of the existing structured sparse HW, i.e. the TASD unit, through RTL prototyping and synthesis with Nangate 15nm Technology Library. We observe up to 2% of the area for all PEs as TASD units are composed of simple comparator trees.

6. Related Work

6.1. SW techniques for structured sparse HW

Since the structured sparse (2:4) accelerator is available in off-the-shelf NVIDIA GPUs with Ampere [46] and Hopper [48] architecture, ample work has focused on exploiting structured sparse acceleration for DNNs.

Solutions with fine-tuning. DominoSearch [62] proposed a method to find layer-wise N:M sparsity during training. Optimal N:M [7] enforces the structured pattern during training, but with a minimum-variance-based pruning method, and applies the structured pattern to input activations. This line of work is orthogonal to our work as we focus on approximating unstructured sparsity without fine-tuning. Fine-tuning will increase the benefit of TASD, as more aggressive approximation can now maintain the same model accuracy. Doping [63] uses an extremely sparse matrix in addition to a compressed matrix derived from Kronecker products to improve the quality of the model, but unlike TASD, it uses the extra extremely sparse matrix to give additional freedom during the training, not for the approximating the given sparse matrix.

Solutions without fine-tuning. SparseTIR [68] introduces composable formats and transformations for sparse compilation of deep learning workloads. However, they have not considered approximating sparse tensors and accelerating DNNs using structured sparse hardware. Another work [52] shows permuting channels in the weight tensors can recover accuracy easily when training N:M sparse networks. TASD is compatible with channel permutation, and we believe combining these two orthogonal techniques will further improve the accuracy of decomposed models with aggressive approximation.

6.2. HW support for sparse DNNs

Sparsity support for DNN inference. Different architectures have been proposed to support for weight sparsity [6, 17, 28, 46], for activation sparsity [26], and more recently, for both [23, 64, 65]. As mentioned earlier, these

accelerators can be broadly classified as structured sparse or unstructured sparse HW. Unstructured sparse HW provides native support for any sparsity pattern but is more costly to build; structured sparse HW is efficient but requires model fine-tuning. TASD bridges the gap in this area by providing an unstructured sparse interface while only requiring structured sparse HW.

Sparsity support for DNN training. Since weight tensors are mostly dense during training, prior work has focused on activation and gradient sparsity during DNN training. The simpler support is to compress sparse activation and gradient, such as CompressDMA [57] and ZComp [3]. These techniques save data movements and memory requirements, but not overall compute. The more complex techniques target reducing computation during training, such as TensorDash [39] and SAVE [18]. However, they need to give up data movement savings for better support for sparse tensor transposition during training. TASD can be used to approximate sparse activations and gradients, too. As prior work [33, 57] has shown that the degree of activation and gradient sparsity stays stable, TASD-A can approximate these dynamic tensors during run-time to enable the efficient structured sparse HW support for sparse training. We leave this to future work.

7. Conclusion

Sparse DNN model developers prefer to induce unstructured sparsity for expressibility, while sparse DNN hardware designers prefer to support structured sparsity for HW efficiency. This mismatch of the desired sparsity pattern prevents sparse DNN acceleration from being widely adopted in practice.

To close the gap, we introduce TASD, a method that approximates an unstructured sparse tensor with a series of structured sparse tensors. Next, we propose a framework, TASDER, which finds TASD configuration for each DNN layer to accelerate off-the-shelf sparse and dense DNNs. To maximize the benefit of TASD, we propose a simple architectural extension and dataflow on top of structured sparse accelerators. TASD improves EDP by up to 83% and 74% on average, while maintaining 99% of the model accuracy without any fine-tuning.

References

- [1] Pytorch torchvision models. <https://pytorch.org/vision/stable/index.html>.
- [2] Artifact: Sparseloop: An Analytical Approach To Sparse Tensor Accelerator Modeling. Zenodo, October 2022. <https://doi.org/10.5281/zenodo.7027215>.
- [3] Berkin Akin, Zeshan A. Chishti, and Alaa R. Alameldeen. Zcomp: Reducing dnn cross-layer memory footprint using vector extensions. In *Proceedings of the 52nd Annual IEEE/ACM International Symposium on Microarchitecture*, MICRO '23, page 126–138, New York, NY, USA, 2019. Association for Computing Machinery.
- [4] Dario Amodei, Sundaram Ananthanarayanan, Rishita Anubhai, Jingliang Bai, Eric Battenberg, Carl Case, Jared Casper, Bryan Catanzaro, Qiang Cheng, Guoliang Chen, et al. Deep speech 2: End-to-end speech recognition in english and mandarin. In *International conference on machine learning*, pages 173–182. PMLR, 2016.
- [5] Tianlong Chen, Xuxi Chen, Xiaolong Ma, Yanzhi Wang, and Zhangyang Wang. Coarsening the granularity: Towards structurally sparse lottery tickets. In *International conference on machine learning*, pages 3025–3039. PMLR, 2022.
- [6] Yu-Hsin Chen, Tien-Ju Yang, Joel Emer, and Vivienne Sze. Eyeriss v2: A flexible accelerator for emerging deep neural networks on mobile devices. *IEEE Journal on Emerging and Selected Topics in Circuits and Systems*, 9(2):292–308, 2019.
- [7] Brian Chmiel, Itay Hubara, Ron Banner, and Daniel Soudry. Optimal fine-grained n: M sparsity for activations and neural gradients. *arXiv preprint arXiv:2203.10991*, 2022.
- [8] Aakanksha Chowdhery, Sharan Narang, Jacob Devlin, Maarten Bosma, Gaurav Mishra, Adam Roberts, Paul Barham, Hyung Won Chung, Charles Sutton, Sebastian Gehrmann, et al. Palm: Scaling language modeling with pathways. *arXiv preprint arXiv:2204.02311*, 2022.
- [9] Özgün Çiçek, Ahmed Abdulkadir, Soeren S Lienkamp, Thomas Brox, and Olaf Ronneberger. 3d u-net: learning dense volumetric segmentation from sparse annotation. In *Medical Image Computing and Computer-Assisted Intervention—MICCAI 2016: 19th International Conference, Athens, Greece, October 17–21, 2016, Proceedings, Part II 19*, pages 424–432. Springer, 2016.
- [10] Tri Dao, Beidi Chen, Kaizhao Liang, Jiaming Yang, Zhao Song, Atri Rudra, and Christopher Re. Pixelated butterfly: Simple and efficient sparse training for neural network models. *arXiv preprint arXiv:2112.00029*, 2021.
- [11] Jia Deng, Wei Dong, Richard Socher, Li-Jia Li, Kai Li, and Li Fei-Fei. Imagenet: A large-scale hierarchical image database. In *2009 IEEE conference on computer vision and pattern recognition*, pages 248–255. Ieee, 2009.
- [12] Jacob Devlin, Ming-Wei Chang, Kenton Lee, and Kristina Toutanova. BERT: Pre-training of deep bidirectional transformers for language understanding. In *Proceedings of the 2019 Conference of the North American Chapter of the Association for Computational Linguistics: Human Language Technologies, Volume 1 (Long and Short Papers)*, pages 4171–4186, Minneapolis, Minnesota, June 2019. Association for Computational Linguistics.
- [13] Alexey Dosovitskiy, Lucas Beyer, Alexander Kolesnikov, Dirk Weissenborn, Xiaohua Zhai, Thomas Unterthiner, Mostafa Dehghani, Matthias Minderer, Georg Heigold, Sylvain Gelly, et al. An image is worth 16x16 words: Transformers for image recognition at scale. *arXiv preprint arXiv:2010.11929*, 2020.
- [14] Chao Fang, Aojun Zhou, and Zhongfeng Wang. An algorithm–hardware co-optimized framework for accelerating n: M sparse transformers. *IEEE Transactions on Very Large Scale Integration (VLSI) Systems*, 30(11):1573–1586, 2022.
- [15] William Fedus, Barret Zoph, and Noam Shazeer. Switch transformers: Scaling to trillion parameter models with simple and efficient sparsity. *arXiv preprint arXiv:2101.03961*, 2021.
- [16] Elias Frantar and Dan Alistarh. Massive language models can be accurately pruned in one-shot. *arXiv preprint arXiv:2301.00774*, 2023.
- [17] Ashish Gondimalla, Mithuna Thottethodi, and T. N. Vijaykumar. Eureka: Efficient tensor cores for one-sided unstructured sparsity in dnn inference. In *Proceedings of the 56th Annual IEEE/ACM International Symposium on Microarchitecture*, MICRO '23, page 324–337, New York, NY, USA, 2023. Association for Computing Machinery.
- [18] Zhangxiaowen Gong, Houxiang Ji, Christopher W. Fletcher, Christopher J. Hughes, Sara Baghsorkhi, and Josep Torrellas. Save: Sparsity-aware vector engine for accelerating dnn training and inference on cpus. In *2020 53rd Annual IEEE/ACM International Symposium on Microarchitecture (MICRO)*, pages 796–810, 2020.
- [19] Song Han, Huizi Mao, and William J Dally. Deep compression: Compressing deep neural networks with pruning, trained quantization and huffman coding. *arXiv preprint arXiv:1510.00149*, 2015.
- [20] Kaiming He, Xiangyu Zhang, Shaoqing Ren, and Jian Sun. Deep residual learning for image recognition. In *Proceedings of the IEEE conference on computer vision and pattern recognition*, pages 770–778, 2016.
- [21] Dan Hendrycks and Kevin Gimpel. Gaussian error linear units (gelus). *arXiv preprint arXiv:1606.08415*, 2016.
- [22] Andrew G Howard, Menglong Zhu, Bo Chen, Dmitry Kalenichenko, Weijun Wang, Tobias Weyand, Marco Andreetto, and Hartwig Adam. Mobilenets: Efficient convolutional neural networks for mobile vision applications. *arXiv preprint arXiv:1704.04861*, 2017.
- [23] Guyue Huang, Zhengyang Wang, Po-An Tsai, Chen Zhang, Yufei Ding, and Yuan Xie. Rm-stc: Row-merge dataflow inspired gpu sparse tensor core for energy-efficient sparse acceleration. In *Proceedings of the 56th Annual IEEE/ACM International Symposium on Microarchitecture*, MICRO '23, page 338–352, New York, NY, USA, 2023. Association for Computing Machinery.

- [24] Qijing Huang, Minwoo Kang, Grace Dinh, Thomas Norell, Aravind Kaliaiah, James Demmel, John Wawrzyniec, and Yakun Sophia Shao. Cosa: Scheduling by constrained optimization for spatial accelerators. In *2021 ACM/IEEE 48th Annual International Symposium on Computer Architecture (ISCA)*, pages 554–566, 2021.
- [25] Itay Hubara, Brian Chmiel, Moshe Island, Ron Banner, Joseph Naor, and Daniel Soudry. Accelerated sparse neural training: A provable and efficient method to find n : m transposable masks. *Advances in neural information processing systems*, 34:21099–21111, 2021.
- [26] Jun-Woo Jang, Sehwan Lee, Dongyoung Kim, Hyunsun Park, Ali Shafiee Ardestani, Yeongjae Choi, Channoh Kim, Yoojin Kim, Hyeonseoek Yu, Hamzah Abdel-Aziz, Jun-Seok Park, Heonsoo Lee, Dongwoo Lee, Myeong Woo Kim, Hanwoong Jung, Heewoo Nam, Dongguen Lim, Seungwon Lee, Joon-Ho Song, Suknam Kwon, Joseph Hassoun, SukHwan Lim, and Changkyu Choi. Sparsity-aware and re-configurable npu architecture for samsung flagship mobile soc. In *2021 ACM/IEEE 48th Annual International Symposium on Computer Architecture (ISCA)*, pages 15–28, 2021.
- [27] Geonhwa Jeong, Sana Damani, Abhimanyu Rajeshkumar Bambhaniya, Eric Qin, Christopher J. Hughes, Sreenivas Subramoney, Hyesoon Kim, and Tushar Krishna. Vegeta: Vertically-integrated extensions for sparse/dense gemm tile acceleration on cpus. In *2023 IEEE International Symposium on High Performance Computer Architecture (HPCA)*, 2023.
- [28] Geonhwa Jeong, Eric Qin, Ananda Samajdar, Christopher J. Hughes, Sreenivas Subramoney, Hyesoon Kim, and Tushar Krishna. Rasa: Efficient register-aware systolic array matrix engine for cpu. In *2021 58th ACM/IEEE Design Automation Conference (DAC)*, pages 253–258, 2021.
- [29] Norman P. Jouppi, Cliff Young, Nishant Patil, David Patterson, Gaurav Agrawal, Raminder Bajwa, Sarah Bates, Suresh Bhatia, Nan Boden, Al Borchers, Rick Boyle, Pierre-luc Cantin, Clifford Chao, Chris Clark, Jeremy Coriell, Mike Daley, Matt Dau, Jeffrey Dean, Ben Gelb, Tara Vazir Ghaemmaghami, Rajendra Gottipati, William Gulland, Robert Hagmann, C. Richard Ho, Doug Hogberg, John Hu, Robert Hundt, Dan Hurt, Julian Ibarz, Aaron Jaffey, Alek Jaworski, Alexander Kaplan, Harshit Khaitan, Daniel Killebrew, Andy Koch, Naveen Kumar, Steve Lacy, James Laudon, James Law, Diemthu Le, Chris Leary, Zhuyuan Liu, Kyle Lucke, Alan Lundin, Gordon MacKean, Adriana Maggiore, Maire Mahony, Kieran Miller, Rahul Nagarajan, Ravi Narayanaswami, Ray Ni, Kathy Nix, Thomas Norrie, Mark Omernick, Narayana Penukonda, Andy Phelps, Jonathan Ross, Matt Ross, Amir Salek, Emad Samadiani, Chris Severn, Gregory Sizikov, Matthew Snelham, Jed Souter, Dan Steinberg, Andy Swing, Mercedes Tan, Gregory Thorson, Bo Tian, Horia Toma, Erick Tuttle, Vijay Vasudevan, Richard Walter, Walter Wang, Eric Wilcox, and Doe Hyun Yoon. In-datasheet performance analysis of a tensor processing unit. *SIGARCH Comput. Archit. News*, 45(2):1–12, jun 2017.
- [30] Alex Krizhevsky, Ilya Sutskever, and Geoffrey E Hinton. Imagenet classification with deep convolutional neural networks. *Advances in neural information processing systems*, 25, 2012.
- [31] Hyoukjun Kwon, Prasanth Chatarasi, Vivek Sarkar, Tushar Krishna, Michael Pellauer, and Angshuman Parashar. Maestro: A data-centric approach to understand reuse, performance, and hardware cost of dnn mappings. *IEEE Micro*, 40(3):20–29, 2020.
- [32] Zonglin Li, Chong You, Srinadh Bhojanapalli, Daliang Li, Ankit Singh Rawat, Sashank Reddi, Ke Ye, Felix Ren chyan Chern, Felix Yu, Ruiqi Guo, and Sanjiv Kumar. On emergence of activation sparsity in trained transformers. In *2023 International Conference on Learning Representations (ICLR)*, 2023.
- [33] Zonglin Li, Chong You, Srinadh Bhojanapalli, Daliang Li, Ankit Singh Rawat, Sashank J Reddi, Ke Ye, Felix Chern, Felix Yu, Ruiqi Guo, et al. Large models are parsimonious learners: Activation sparsity in trained transformers. *arXiv preprint arXiv:2210.06313*, 2022.
- [34] Tsung-Yi Lin, Priya Goyal, Ross Girshick, Kaiming He, and Piotr Dollár. Focal loss for dense object detection. In *Proceedings of the IEEE international conference on computer vision*, pages 2980–2988, 2017.
- [35] Zhi-Gang Liu, Paul N. Whatmough, and Matthew Mattina. Systolic tensor array: An efficient structured-sparse gemm accelerator for mobile cnn inference. *IEEE Computer Architecture Letters*, 19(1):34–37, 2020.
- [36] Zhi-Gang Liu, Paul N Whatmough, Yuhao Zhu, and Matthew Mattina. S2ta: Exploiting structured sparsity for energy-efficient mobile cnn acceleration. *arXiv preprint arXiv:2107.07983*, 2021.
- [37] Zhi-Gang Liu, Paul N. Whatmough, Yuhao Zhu, and Matthew Mattina. S2ta: Exploiting structured sparsity for energy-efficient mobile cnn acceleration. In *2022 IEEE International Symposium on High Performance Computer Architecture (HPCA)*, 2022.
- [38] Zhuang Liu, Hanzi Mao, Chao-Yuan Wu, Christoph Feichtenhofer, Trevor Darrell, and Saining Xie. A convnet for the 2020s. In *Proceedings of the IEEE/CVF Conference on Computer Vision and Pattern Recognition*, pages 11976–11986, 2022.
- [39] Mostafa Mahmoud, Isak Edo, Ali Hadi Zadeh, Omar Mohamed Awad, Gennady Pekhimenko, Jorge Albericio, and Andreas Moshovos. Tensordash: Exploiting sparsity to accelerate deep neural network training. In *2020 53rd Annual IEEE/ACM International Symposium on Microarchitecture (MICRO)*, pages 781–795, 2020.
- [40] Linyan Mei, Pouya Houshmand, Vikram Jain, Sebastian Giraldo, and Marian Verhelst. Zigzag: Enlarging joint architecture-mapping design space exploration for dnn accelerators. *IEEE Transactions on Computers*, 70(8):1160–1174, 2021.
- [41] Asit Mishra, Jorge Albericio Latorre, Jeff Pool, Darko Stosic, Dusan Stosic, Ganesh Venkatesh, Chong Yu, and Paulius Micikevicius. Accelerating sparse deep neural networks. *arXiv preprint arXiv:2104.08378*, 2021.
- [42] Pavlo Molchanov, Jimmy Hall, Hongxu Yin, Jan Kautz, Nicolo Fusi, and Arash Vahdat. Lana: Latency-aware network acceleration. In *European Conference on Computer Vision*, pages 137–156. Springer, 2022.
- [43] Sharan Narang, Eric Undersander, and Gregory Diamos. Block-sparse recurrent neural networks. *arXiv preprint arXiv:1711.02782*, 2017.
- [44] Maxim Naumov, Dheevatsa Mudigere, Hao-Jun Michael Shi, Jianyu Huang, Narayanan Sundaraman, Jongsoo Park, Xiaodong Wang, Udit Gupta, Carole-Jean Wu, Alisson G Azzolini, et al. Deep learning recommendation model for personalization and recommendation systems. *arXiv preprint arXiv:1906.00091*, 2019.
- [45] Neuralmagic. Sparsezoo models, 2023. <https://sparsezoo.neuralmagic.com/>.
- [46] NVIDIA. Nvidia ampere ga102 gpu architecture, 2020. <https://www.nvidia.com/content/PDF/nvidia-ampere-ga-102-gpu-architecture-whitepaper-v2.1.pdf>.
- [47] NVIDIA. Nvidia v100 tensor core gpu, 2020. <https://images.nvidia.com/content/technologies/volta/pdf/volta-v100-datasheet-update-us-1165301-r5.pdf>.
- [48] NVIDIA. Nvidia h100 tensor core gpu architecture, 2022. <https://resources.nvidia.com/en-us-tensor-core>.
- [49] Angshuman Parashar, Priyanka Raina, Yakun Sophia Shao, Yu-Hsin Chen, Victor A. Ying, Anurag Mukkara, Rangharajan Venkatesan, Brucek Khailany, Stephen W. Keckler, and Joel Emer. Timeloop: A systematic approach to dnn accelerator evaluation. In *2019 IEEE International Symposium on Performance Analysis of Systems and Software (ISPASS)*, pages 304–315, 2019.
- [50] Angshuman Parashar, Minsoo Rhu, Anurag Mukkara, Antonio Puglielli, Rangharajan Venkatesan, Brucek Khailany, Joel Emer, Stephen W. Keckler, and William J. Dally. Senn: An accelerator for compressed-sparse convolutional neural networks. In *2017 ACM/IEEE 44th Annual International Symposium on Computer Architecture (ISCA)*, pages 27–40, 2017.
- [51] Adam Paszke, Sam Gross, Francisco Massa, Adam Lerer, James Bradbury, Gregory Chanan, Trevor Killeen, Zeming Lin, Natalia Gimelshein, Luca Antiga, Alban Desmaison, Andreas Kopf, Edward Yang, Zachary DeVito, Martin Raison, Alykhan Tejani, Sasank Chilamkurthy, Benoit Steiner, Lu Fang, Junjie Bai, and Soumith Chintala. Pytorch: An imperative style, high-performance deep learning library. In H. Wallach, H. Larochelle, A. Beygelzimer, F. d’Alché-Buc, E. Fox, and R. Garnett, editors, *Advances in Neural Information Processing Systems* 32, pages 8024–8035. Curran Associates, Inc., 2019.
- [52] Jeff Pool and Chong Yu. Channel permutations for $n:m$ sparsity. In *Advances in Neural Information Processing Systems*, volume 34, pages 13316–13327. Curran Associates, Inc., 2021.
- [53] Eric Qin, Ananda Samajdar, Hyoukjun Kwon, Vineet Nadella, Sudarshan Srinivasan, Dipankar Das, Bharat Kaul, and Tushar Krishna. Sigma: A sparse and irregular gemm accelerator with flexible interconnects for dnn training. In *2020 IEEE International Symposium on High Performance Computer Architecture (HPCA)*, pages 58–70, 2020.
- [54] Alec Radford, Jeffrey Wu, Rewon Child, David Luan, Dario Amodei, Ilya Sutskever, et al. Language models are unsupervised multitask learners. *OpenAI blog*, 1(8):9, 2019.
- [55] Prajit Ramachandran, Barret Zoph, and Quoc V Le. Searching for activation functions. *arXiv preprint arXiv:1710.05941*, 2017.
- [56] Vijay Janapa Reddi, Christine Cheng, David Kanter, Peter Mattson, Guenther Schmuelling, Carole-Jean Wu, Brian Anderson, Maximilien Breughe, Mark Charlebois, William Chou, Ramesh Chukka, Cody Coleman, Sam Davis, Pan Deng, Greg Diamos, Jared Duke, Dave Fick, J. Scott Gardner, Itay Hubara, Sachin Idgunji, Thomas B. Jablin, Jeff

- Jiao, Tom St. John, Pankaj Kanwar, David Lee, Jeffery Liao, Anton Lokhmotov, Francisco Massa, Peng Meng, Paulius Micikevicius, Colin Osborne, Gennady Pekhimenko, Arun Tejusve Raghunath Rajan, Dilip Sequeira, Ashish Sirasao, Fei Sun, Hanlin Tang, Michael Thomson, Frank Wei, Ephrem Wu, Lingjie Xu, Koichi Yamada, Bing Yu, George Yuan, Aaron Zhong, Peizhao Zhang, and Yuchen Zhou. Mlperf inference benchmark. In *Proceedings of the ACM/IEEE 47th Annual International Symposium on Computer Architecture, ISCA '20*, page 446–459. IEEE Press, 2020.
- [57] Minsoo Rhu, Mike O'Connor, Niladrish Chatterjee, Jeff Pool, Youngeun Kwon, and Stephen W. Keckler. Compressing dma engine: Leveraging activation sparsity for training deep neural networks. In *2018 IEEE International Symposium on High Performance Computer Architecture (HPCA)*, pages 78–91, 2018.
- [58] Ananda Samajdar, Jan Moritz Joseph, Yuhao Zhu, Paul Whatmough, Matthew Mattina, and Tushar Krishna. A systematic methodology for characterizing scalability of dnn accelerators using scale-sim. In *2020 IEEE International Symposium on Performance Analysis of Systems and Software (ISPASS)*, pages 58–68, 2020.
- [59] Jong Hoon Shin, Ali Shafiee, Ardavan Pedram, Hamzah Abdel-Aziz, Ling Li, and Joseph Hassoun. Design space exploration of sparse accelerators for deep neural networks. *arXiv preprint arXiv:2107.12922*, 2021.
- [60] Mohammad Shoeybi, Mostofa Patwary, Raul Puri, Patrick LeGresley, Jared Casper, and Bryan Catanzaro. Megatron-lm: Training multi-billion parameter language models using model parallelism. *arXiv preprint arXiv:1909.08053*, 2019.
- [61] David R So, Wojciech Mańke, Hanxiao Liu, Zihang Dai, Noam Shazeer, and Quoc V Le. Primer: Searching for efficient transformers for language modeling. *arXiv preprint arXiv:2109.08668*, 2021.
- [62] Wei Sun, Aojun Zhou, Sander Stuijk, Rob Wijnhoven, Andrew Oakleigh Nelson, hongsheng Li, and Henk Corporaal. Dominosearch: Find layer-wise fine-grained n:m sparse schemes from dense neural networks. In M. Ranzato, A. Beygelzimer, Y. Dauphin, P.S. Liang, and J. Wortman Vaughan, editors, *Advances in Neural Information Processing Systems*, volume 34, pages 20721–20732. Curran Associates, Inc., 2021.
- [63] Urmish Thakker, Paul Whatmough, Zhigang Liu, Matthew Mattina, and Jesse Beu. Doping: A technique for extreme compression of lstm models using sparse structured additive matrices. *Proceedings of machine learning and systems*, 3:533–549, 2021.
- [64] Yang Wang, Chen Zhang, Zhiqiang Xie, Cong Guo, Yunxin Liu, and Jingwen Leng. Dual-side sparse tensor core. In *Proceedings of the 48th Annual International Symposium on Computer Architecture, ISCA '21*, page 1083–1095. IEEE Press, 2021.
- [65] Yannan Nellie Wu, Po-An Tsai, Saurav Muralidharan, Angshuman Parashar, Vivienne Sze, and Joel Emer. Highlight: Efficient and flexible dnn acceleration with hierarchical structured sparsity. In *Proceedings of the 56th Annual IEEE/ACM International Symposium on Microarchitecture, MICRO '23*, page 1106–1120, New York, NY, USA, 2023. Association for Computing Machinery.
- [66] Yannan Nellie Wu, Po-An Tsai, Angshuman Parashar, Vivienne Sze, and Joel S. Emer. Sparseloop: An analytical approach to sparse tensor accelerator modeling. In *2022 55th IEEE/ACM International Symposium on Microarchitecture (MICRO)*, pages 1377–1395, 2022.
- [67] Amir Yazdanbakhsh, Sheng-Chun Kao, Shivani Agrawal, Suvinay Subramanian, Tushar Krishna, and Utku Evci. Training recipe for n:m structured sparsity with decaying pruning mask, 2022.
- [68] Zihao Ye, Ruihang Lai, Junru Shao, Tianqi Chen, and Luis Ceze. Sparsedir: Composable abstractions for sparse compilation in deep learning. In *Proceedings of the 28th ACM International Conference on Architectural Support for Programming Languages and Operating Systems, Volume 3, ASPLOS 2023*, page 660–678, New York, NY, USA, 2023. Association for Computing Machinery.
- [69] Manzil Zaheer, Guru Guruganesh, Kumar Avinava Dubey, Joshua Ainslie, Chris Alberti, Santiago Ontanon, Philip Pham, Anirudh Ravula, Qifan Wang, Li Yang, et al. Big bird: Transformers for longer sequences. *Advances in neural information processing systems*, 33:17283–17297, 2020.
- [70] Yuxin Zhang, Mingbao Lin, Zhihang Lin, Yiting Luo, Ke Li, Fei Chao, Yongjian Wu, and Rongrong Ji. Learning best combination for efficient n: M sparsity. *Advances in Neural Information Processing Systems*, 35:941–953, 2022.
- [71] Aojun Zhou, Yukun Ma, Junnan Zhu, Jianbo Liu, Zhijie Zhang, Kun Yuan, Wenxiu Sun, and Hongsheng Li. Learning n:m fine-grained structured sparse neural networks from scratch. In *International Conference on Learning Representations*, 2021.
- [72] Maohua Zhu, Tao Zhang, Zhenyu Gu, and Yuan Xie. Sparse tensor core: Algorithm and hardware co-design for vector-wise sparse neural networks on modern gpus. In *Proceedings of the 52nd Annual IEEE/ACM International Symposium on Microarchitecture, MICRO '22*, page 359–371, New York, NY, USA, 2019. Association for Computing Machinery.